Simultaneous measurement of β-delayed proton and γ emission of ^{26}P for the ^{25}Al(p,γ) ^{26}Si reaction rate

P. F. Liang (梁鹏飞),[1,*] L. J. Sun (孙立杰),[2,3,*] J. Lee (李晓菁),[1,†] S. Q. Hou (侯素青),[4] X. X. Xu (徐新星),[1,2,4,‡] C. J. Lin (林承键),[2,5,§] C. X. Yuan (袁岑溪),[6] J. J. He (何建军),[7,8] Z. H. Li (李智焕),[9] J. S. Wang (王建松),[10,4,8] D. X. Wang (王东玺),[2] H. Y. Wu (吴鸿毅),[9] Y. Y. Yang (杨彦云),[4] Y. H. Lam (蓝乙华),[4] P. Ma (马朋),[4] F. F. Duan (段芳芳),[11,4] Z. H. Gao (高志浩),[4,11] Q. Hu (胡强),[4] Z. Bai (白真),[4] J. B. Ma (马军兵),[4] J. G. Wang (王建国),[4] F. P. Zhong (钟福鹏),[2,5] C. G. Wu (武晨光),[9] D. W. Luo (罗迪雯),[9] Y. Jiang (蒋颖),[9] Y. Liu (刘洋),[9] D. S. Hou (侯东升),[4,8] R. Li (李忍),[4,8] N. R. Ma (马南茹),[2] W. H. Ma (马维虎),[4,12] G. Z. Shi (石国柱),[4] G. M. Yu (余功明),[4] D. Patel,[4] S. Y. Jin (金树亚),[4,8] Y. F. Wang (王煜峰),[13,4] Y. C. Yu (余悦超),[13,4] Q. W. Zhou (周清武),[14,4] P. Wang (王鹏),[14,4] L. Y. Hu (胡力元),[15] X. Wang (王翔),[9] H. L. Zang (臧宏亮),[9] P. J. Li (李朋杰),[1] Q. Q. Zhao (赵青青),[1] H. M. Jia (贾会明),[2] L. Yang (杨磊),[2] P. W. Wen (温培威),[2] F. Yang (杨峰),[2] G. L. Zhang (张高龙),[16] M. Pan (潘敏),[16,2] X. Y. Wang (汪小雨),[16] H. H. Sun (孙浩翰),[2] Z. G. Hu (胡正国),[4] R. F. Chen (陈若富),[4] M. L. Liu (柳敏良),[4] W. Q. Yang (杨维青),[4] and Y. M. Zhao (赵玉民)[3]

(RIBLL Collaboration)

[1]*Department of Physics, The University of Hong Kong, Hong Kong, China*
[2]*Department of Nuclear Physics, China Institute of Atomic Energy, Beijing 102413, China*
[3]*School of Physics and Astronomy, Shanghai Jiao Tong University, Shanghai 200240, China*
[4]*Institute of Modern Physics, Chinese Academy of Sciences, Lanzhou 730000, China*
[5]*College of Physics and Technology, Guangxi Normal University, Guilin 541004, China*
[6]*Sino-French Institute of Nuclear Engineering and Technology, Sun Yat-Sen University, Zhuhai 519082, China*
[7]*College of Nuclear Science and Technology, Beijing Normal University, Beijing 100875, China*
[8]*University of Chinese Academy of Sciences, Beijing 100049, China*
[9]*State Key Laboratory of Nuclear Physics and Technology, School of Physics, Peking University, Beijing 100871, China*
[10]*School of Science, Huzhou University, Huzhou 313000, China*
[11]*School of Nuclear Science and Technology, Lanzhou University, Lanzhou 730000, China*
[12]*Institute of Modern Physics, Fudan University, Shanghai 200433, China*
[13]*School of Physics and Astronomy, Yunnan University, Kunming 650091, China*
[14]*School of Physical Science and Technology, Southwest University, Chongqing 400044, China*
[15]*Fundamental Science on Nuclear Safety and Simulation Technology Laboratory, Harbin Engineering University, Harbin 150001, China*
[16]*School of Physics and Nuclear Energy Engineering, Beihang University, Beijing 100191, China*

(Received 21 October 2019; accepted 13 January 2020; published 14 February 2020)

The β decay of ^{26}P was used to populate the astrophysically important $E_x = 5929.4(8)$ keV, $J^\pi = 3^+$ state of ^{26}Si. Both β-delayed protons at 418(8) keV and γ rays at 1742(2) keV emitted from this state were measured simultaneously for the first time, and the corresponding absolute intensities have been estimated as 11.1(12)% and 0.59(44)%, respectively. The half-life of ^{26}P has been determined to be 43.6(3) ms, which is in good agreement with previous experimental results. Besides, shell-model calculations with weakly bound effects were performed to investigate the decay properties of other resonant states and a spin-parity of 4^+ rather than 0^+ is favored for the $E_x = 5945.9(40)$ keV state. Combining the experimental results and theoretical calculations, the ^{25}Al(p,γ) ^{26}Si reaction rate in explosive hydrogen burning environments was calculated. The new determined total reaction rate is consistent with previous studies at $T > 0.2$ GK.

DOI: 10.1103/PhysRevC.101.024305

I. INTRODUCTION

As the half-life of ^{26}Al ($T_{1/2} = 7.17 \times 10^5$ yr) is much less than the age of the galaxy ($\approx 10^{10}$ yr), the observation of 1809-keV γ ray from β decay of ^{26}Al could directly prove that the stellar nucleosynthesis processes are currently active in our galaxy. In previous satellite-based astronomical observations, the mass of galactic ^{26}Al was estimated to be 2.7 ± 0.7 solar masses ($M_\odot$) [1,2]. The primary sites of

*These authors contributed equally to this work and should be considered as co-first authors.
†jleehc@hku.hk
‡xinxing@impcas.ac.cn
§cjlin@ciae.ac.cn

galactic ^{26}Al were suggested to be massive stars and core-collapse supernovae concluded from the spatial distribution of ^{26}Al [3,4]. However, the observed ^{60}Fe / ^{26}Al γ-ray flux ratio [5,6] is smaller than theoretical predictions, which indicates that there should be other important sources for galactic ^{26}Al [7,8]. As one of the most frequent types of thermonuclear stellar explosions in the galaxy, classical novae are expected to contribute 0.1–0.4 $M_\odot$ of galactic ^{26}Al [9,10], or even up to 0.6 $M_\odot$ [11]. In outbursts of classical novae (typical temperature of 0.1 GK $< T <$ 0.4 GK), ^{26}Al is produced by the reaction chain ^{24}Mg(p,γ) ^{25}Al(β^+) ^{25}Mg(p,γ) ^{26}Al, which, however, could be bypassed via the proton capture reaction of ^{25}Al(p,γ) ^{26}Si at high temperature (for example, $T > 0.27$ GK [12]), because the isomeric state ^{26}Al^m rather than the ground state ^{26}Al^g is predominantly populated by the subsequent β decay of ^{26}Si [12,13]. Thus, a reliable measurement of the proton-capture reaction rate of ^{25}Al is of great importance to better understand the origin of galactic ^{26}Al.

Direct measurement of the ^{25}Al(p,γ) ^{26}Si reaction cross section may give the most reliable information on the reaction rate, but current available beam intensity of ^{25}Al is not sufficient to perform such a measurement. Indirect measurements combined with theoretical calculations have been therefore conducted. The spin-parity of the ^{25}Al ground state is $J^\pi = \frac{5}{2}^+$ [14], and previous studies convinced us that there are four important resonant states, namely, $E_x = 5676.2(3)$ keV, $J^\pi = 1^+$; $E_x = 5890.1(3)$ keV, $J^\pi = 0^+$; $E_x = 5929.4(8)$ keV, $J^\pi = 3^+$; and $E_x = 5945.9(40)$ keV, $J^\pi = (0^+)$, which lie within 500 keV above the proton threshold of ^{26}Si [$S_p = 5514.0(1)$ keV] [14,15], that could contribute to the ^{25}Al(p,γ) ^{26}Si reaction rate in explosive hydrogen burning environments of classical novae [12,13,16–21]. In fact, crucial resonance information including decay properties of the $E_x = 5929.4(8)$ keV state and the spin-parity assignment of the $E_x = 5945.9(40)$ keV state are still under debate [21,22]. For the $E_x = 5929.4(8)$ keV state, the β decay of ^{26}P was measured to study the decay properties. In 2013, Bennett *et al.* [11] observed the β-delayed γ ray of 1742 keV emitted from the $E_x = 5929.4(8)$ keV state with a $\beta\gamma$ intensity of $[0.18 \pm 0.05(\text{stat.}) \pm 0.04(\text{lit.})]\%$. Based on the experimentally determined absolute βp intensity of $I_p = 17.96(90)\%$ by Thomas *et al.* [23] and the proton-decay partial width of $\Gamma_p = 2.9(10)$ eV by Peplowski *et al.* [13], the partial width of γ decay was derived to be $\Gamma_\gamma = 40 \pm 11(\text{stat.})^{+19}_{-18}(\text{lit.})$ meV from the relation of $I_p/I_\gamma = \Gamma_p/\Gamma_\gamma$. However, a recent study [22], in which a background-free proton spectrum was acquired using an optical time projection chamber, reported an inconsistent value of I_p between 10.4(9)% and 13.8(10)% for βp intensity. Because this state is expected to dominate the total reaction rate in high-temperature environments [12], further experimental investigations should be done to determine the accurate decay information. For the $E_x = 5945.9(40)$ keV state, the spin-parity was reported to be 0^+ based on the comparison between measured differential cross sections and Hauser-Feshbach calculated cross sections in the measurement of the ^{24}Mg$(^3\text{He},n)$ reaction [17]. Later in Refs. [19,20], another state at $E_x = 5890.1(3)$ keV was unambiguously identified with the spin-parity of 0^+ by γ-γ angular correlation measurements. However, the existence of two 0^+ states within this resonance energy region was not supported by either shell-model calculations or mirror-symmetry analysis. In a recent compilation [21], Chipps gave a detailed discussion for this puzzle and pointed out that the 0^+ assignment for both states was possible if one is due to particles being excited into a different shell. This speculation inspired us to perform shell-model calculations with and without taking into account the cross-shell excitations to explore the spin-parity assignment and decay properties of the $E_x = 5945.9(40)$ keV state.

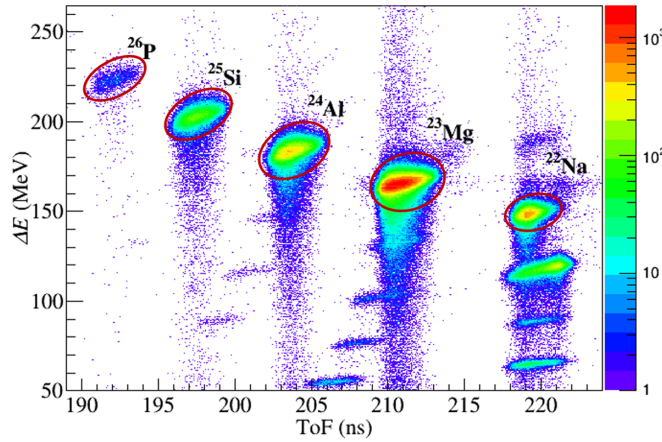

FIG. 1. ToF-ΔE two-dimensional spectrum measured by the plastic scintillators (T1 and T2) and one of the quadrant silicon detectors ($\Delta E1$). Heavy ions are marked with red (gray) circles and the corresponding isotope symbols. The color scale represents the number of ions.

In the present work, the β decay of ^{26}P is used to study the decay properties of the $E_x = 5929.4(8)$ keV state. The βp and $\beta\gamma$ intensities are measured simultaneously to reduce the uncertainties caused by different experimental setups. Besides, shell-model calculations with weakly bound effects are also performed to study the spin-parity assignment of the $E_x = 5945.9(40)$ keV state and the decay information of other resonant states. Combining the experimental results and the theoretical calculations, the proton-capture reaction rate of ^{25}Al(p,γ) ^{26}Si is investigated and compared with previous studies.

II. EXPERIMENTAL TECHNIQUES

The experiment was carried out at the Heavy Ion Reaction Facility in Lanzhou (HIRFL) [24]. A 80.6 MeV/nucleon ^{32}S^{16+} primary beam was produced by the K69 Sector Focus Cyclotron and the K450 Separate Sector Cyclotron and then impinged upon a 1581-μm-thick ^{9}Be target to produce the secondary radioactive ions that were in-flight separated and purified by the Radioactive Ion Beam Line in Lanzhou (RIBLL1) [25]. Heavy ions were identified by the time-of-flight (ToF) and energy loss method event-by-event under a certain magnet rigidity. Figure 1 shows the particle identification two-dimensional spectrum obtained by the two plastic

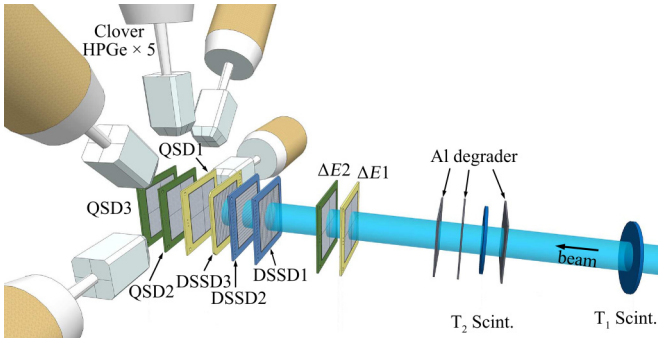

FIG. 2. Schematic layout of the detection setup.

scintillators (T1 and T2 in Fig. 2) and one of the quadrant silicon detectors ($\Delta E1$ in Fig. 2). Different heavy ions are marked with red circles and the corresponding isotope symbols, and ^{26}P heavy ions are clearly distinguished from the contaminations. During the total beam time of about 95.3 h, an average intensity of about one particle per second of ^{26}P ions was delivered to the detection system.

As shown in Fig. 2, a detection system, including three double-sided silicon strip detectors (DSSDs), five Clover-type high-purity germanium (HPGe) detectors, and five quadrant silicon detectors (QSDs), was placed at the last focal plane (T2) of RIBLL1 for the heavy-ion implantation and the measurement of the subsequent decay. The basic techniques of the detection system are described in Refs. [26–28]. Charged particles emitted in the decay of ^{26}P, such as protons and β particles, were measured by the time and position correlations between implantation and decay signals [26–34] with three W1-type DSSDs of different thicknesses (DSSD1 of 142 μm, DSSD2 of 40 μm, and DSSD3 of 304 μm) that were produced by Micron Semiconductor Ltd. For each DSSD, there were 16 vertical and horizontal strips on each side and the width of each strip was 3.1 mm. The thinnest silicon detector, DSSD2, which was installed between DSSD1 and DSSD3, was mainly used to detect low-energy protons for reducing the proton peak shifts due to the β-summing effect [35,36]. The thicker ones, DSSD1 and DSSD3, were employed for the measurement of high-energy protons and β particles. At the upstream of the DSSD array, two of the QSDs ($\Delta E1$ and $\Delta E2$ in Fig. 2) with thicknesses of 309 and 300 μm, respectively, were applied to detect the energy loss of the heavy ions for particle identification. At the downstream of the DSSD array, another three QSDs (QSD1, QSD2, and QSD3 in Fig. 2) with the corresponding thicknesses of 1546, 300, and 300 μm were installed to detect β particles and light contaminations in the beam, such as ^{1}H, ^{3}He, and ^{4}He, for background reduction. The active area of all the QSDs was 5 cm × 5 cm. Around the DSSD array, five HPGe detectors were used to measure the γ rays during the β decay of ^{26}P. In addition to the detectors mentioned, nine movable aluminum degraders with different thicknesses were assembled to reduce the beam energy. In the experiment, the total thickness of the aluminum degraders was set to be 220 μm, which ensured that most of the ^{26}P heavy ions could be stopped by the DSSDs. Totally, about 3.0×10^5 ^{26}P ions were implanted into the DSSD array with proportions

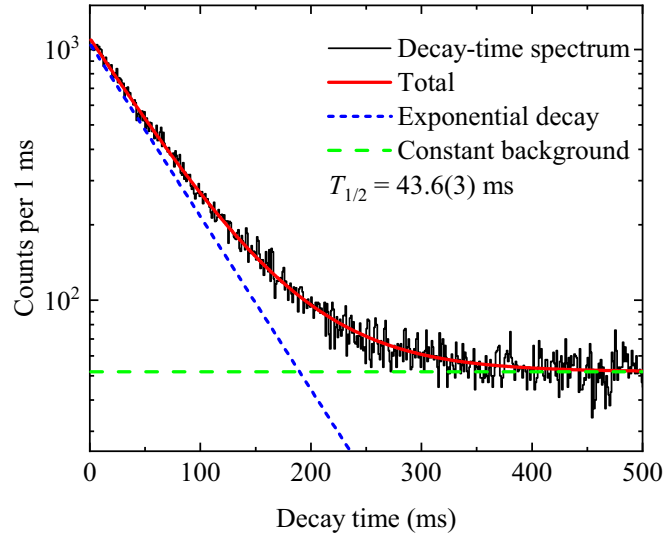

FIG. 3. The decay-time spectrum of ^{26}P was obtained by the time differences between the implantation of ^{26}P and all the subsequent decay events within a time window of 500 ms. An exponential decay component (blue short-dashed line) and a constant background component (green long-dashed line) are applied in the fitting to determine the half-life and estimate the background.

of 2.1%, 45.5%, and 52.4% in DSSD1, DSSD2, and DSSD3, respectively.

III. ANALYSIS AND RESULTS

A. Half-life of ^{26}P

As mentioned in Sec. II, each of the three DSSDs could be divided into 256 pixels by the vertical and horizontal strips. For all 256 × 3 pixels, the time differences between the implantation of ^{26}P and all the subsequent β-delayed charged-particle decay events in the same pixel were measured as the cumulated decay-spectrum shown in Fig. 3. The true correlated implantation and decay events follow an exponential decay curve while the randomly correlated events contribute to a constant background in the spectrum. As a result, the decay-time spectrum can be fitted with an exponential decay component to determine the half-life of ^{26}P and a constant component to estimate the background. Anticoincidence from the QSDs at the downstream of the DSSD array is also applied to reduce the background from light nuclei in the beam. In the present work, the half-life of ^{26}P is measured to be $T_{1/2}$ = 43.6(3) ms, which is in good agreement with literature value of 43.7(6) ms given by Thomas *et al.* [23]. The uncertainty of our result is directly derived from the fitting of the decay-time spectrum.

B. βp and $\beta\gamma$ intensities

In the experiment, remarkably similar implantation distributions of ^{25}Si and ^{26}P in the DSSDs were found and Monte Carlo simulation showed that the systematic uncertainty associated with this difference was expected to be negligible. As a result, the energy calibration and the

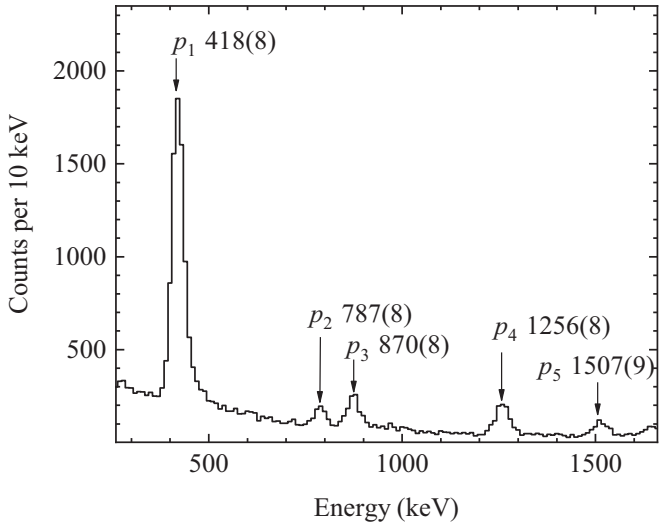

FIG. 4. Low-energy part of the cumulative β-delayed charged-particle spectrum from the β decay of ^{26}P. Proton peaks are labeled as p_1 to p_5 with the corresponding center-of-mass energy in keV. The β pile-up effects are strongly suppressed by the anticoincidence of β signals from QSD1.

detection efficiency calibration of the DSSD array could be performed by an inner-source method with the well-studied β-delayed protons from the decay of ^{25}Si [23]. The adopted energy and corresponding absolute intensity of proton peaks are 401(1) keV [4.75(32%)], 943(2) keV [1.63(20)%], 1804(8) keV [0.58(13)%], 1917(2) keV [2.24(21)%], 2162(4) keV [1.73(22)%], 2307(4) keV [1.57(21)%], 3463(3) keV [2.68(26)%], 4252(2) keV [9.54(66)%], and 5624(3) keV [2.39(20)%] [23]. Figure 4 displays the low-energy part of the cumulative charged-particle spectrum, as the peak labeled as p_1 represents the β-delayed protons emitted from the $E_x =$ 5929.4(8) keV state of ^{26}Si to the ground state of ^{25}Al, which can be used to calculate the resonance energy and the partial width. The β particle in QSD1 is applied as anticoincidence to suppress the β pile-up effects, thus improving the energy resolution of the proton peaks. The center-of-mass energy of the first proton peak is determined to be $p_1 = 418(8)$ keV, which is consistent with literature values of 412(2) keV [23] and 426(30) keV [22] and the derived value of 415.4(8) keV from the databases [14,15]. The uncertainty of the proton peak energy includes the statistical uncertainty of 0.33 keV from the fitting of spectra and the systematic uncertainty of 7.25 keV that is attributed to calibration.

In the present work, the absolute intensity of p_1 is measured to be $I_{p1} = 11.1(12)\%$, which is in good agreement with a recent study between 10.4(9)% and 13.8(10)% [22], but inconsistent with the value of 17.96(90)% in Ref. [23] as shown in the second column of Table I. The uncertainty here is mainly caused by the statistical uncertainty of 0.15% and the systematic uncertainties of 1.14% from the calibration. Other proton peaks at $p_2 = 787(8)$ keV, $p_3 = 870(8)$ keV, $p_4 = 1256(8)$ keV, and $p_5 = 1507(9)$ keV are all observed clearly with corresponding absolute intensities of 0.74(17)%, 1.44(30)%, 1.45(21)%, and 0.80(18)%, respectively.

For HPGe detectors, the energy calibration and the intrinsic detection efficiency calibration were performed with four standard sources: ^{152}Eu, ^{133}Ba, ^{60}Co, and ^{137}Cs. Because ^{22}Al was also studied with the same detection configurations in the experiment, the absolute detection efficiency could be deduced by the β-delayed γ-ray transitions with known energies and absolute intensities of 988 keV [5.7(3)%] and 1796 keV [58(3)%] from ^{26}P [37]; 452 keV [18.4(42)%], 493 keV [15.3(34)%], 945 keV [10.4(23)%], and 1612 keV [15.2(32)%] from ^{25}Si [23]; and 1248.5 keV [38.2(69)%], 1985.6 keV [31.1(54)%]), and 2062.3 keV [34.1(58)%] from ^{22}Al [38]. Figure 5(a) shows the low-background γ-ray spectrum measured by the HPGe detectors in coincidence with the β signals of ^{26}P in DSSD3. Strong γ-ray transitions at 987 keV ($2_2^+ \rightarrow 2_1^+$) and 1797 keV [$2_1^+ \rightarrow 0_1^+$(g.s.)] and also the γ-ray transitions with weak intensities, such as 968 keV ($3_1^+ \rightarrow 2_2^+$), 1400 keV ($3_2^+ \rightarrow 2_2^+$), 1329 keV ($4_4^+ \rightarrow 3_2^+$), and 1532 keV ($4_3^+ \rightarrow 3_1^+$), can be observed clearly in the spectrum. The zoomed-in spectrum with the energy region from 1720 to 1780 keV is shown in Fig. 5(b). γ_1 is the transition from the 3_3^+ [$E_x = 5929.4(8)$ keV] state to the 3_2^+ state and the energy is measured to be $\gamma_1 = 1742(2)$ keV in this work. Here the uncertainty is the quadratic sum of statistical uncertainty of 1.1 keV from the peak and systematical uncertainties of 1.5 keV from the calibration. A constant flat background is estimated for the spectrum and the intensity of γ_1 is determined to be $I_{\gamma_1} = 0.59(44)\%$, where the uncertainty is the quadratic sum of statistical uncertainty of 0.43% from the counts and systematic uncertainties of 0.09% from the calibration. The present result is consistent with previous studies of $I_{\gamma_1} = [0.18 \pm 0.05(\text{stat}) \pm 0.04(\text{lit.})]\%$ in

TABLE I. Decay properties of the $E_x = 5929.4(8)$ keV 3^+ state of ^{26}Si from this work and previous studies.

Reference	I_{p1}(%) [418(8) keV]	$I_{\gamma 1}$(%) [1742(2) keV]	Γ_p (eV)[a]	Γ_γ (eV)
This work	11.1(12)	0.59(44)	2.9(10)	$6.04^{+3.00}_{-2.76} \times 10^{-2}$[b]
Thomas *et al.* [23]	17.96(90)			
Janiak *et al.* [22]	10.4(9)–13.8(10)			
		[0.18 ± 0.05 (stat.)		[4.0 ± 1.1 (stat.)
Bennett *et al.* [11]			2.9(10)	
		±0.04 (lit.)]		$^{+1.9}_{-1.8}$(lit.)] × 10^{-2}
Pérez-Loureiro [37]		0.15(5)		

[a]Adopted value in Ref. [13].
[b]The error-weighted mean value of $I_{\gamma 1} = 0.16(4)\%$ was used here to determine Γ_γ.

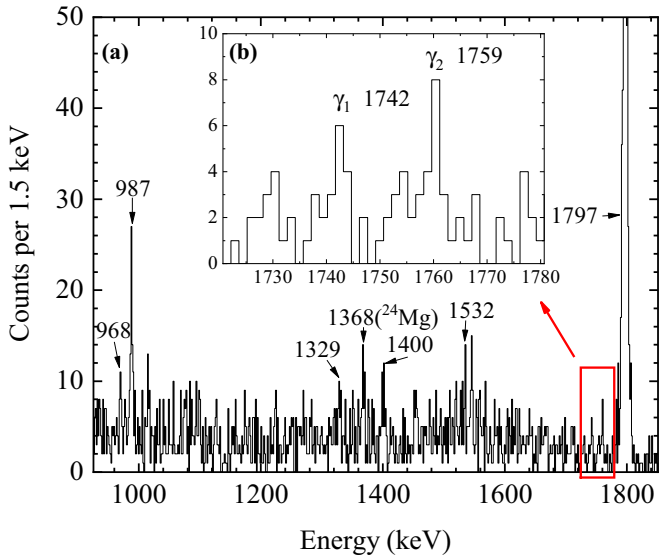

FIG. 5. (a) The cumulative γ-ray spectrum measured by HPGe detectors that are gated by the β particles in DSSD3. (b) γ-ray spectrum from 1720 to 1780 keV.

Ref. [11] and $I_{\gamma_1} = 0.15(5)\%$ in Ref. [37] as presented in the third column of Table I. The peak labeled as γ_2 represents the transition from the 4_4^+ state to the 3_1^+ state, and the energy and intensity are determined to be $\gamma_2 = 1759(2)$ keV and $I_{\gamma_2} = 0.86(51)\%$, respectively. Another peak at around 1730 keV is the double-escape peak of ^{24}Mg, which was also observed in Refs. [11,37]. The partial γ-decay branch of the 1742(2) keV γ ray from the $E_x = 5929.4(8)$ keV, $J^\pi = 3^+$ level was expected to be $71^{+13}_{-19}\%$ based on the mirror transition of ^{26}Mg [11,16]. Adopting this assumption and using the error-weighted mean value of $I_{\gamma 1} = 0.16(4)\%$ from this work and Refs. [11,37], the total $\beta\gamma$ intensity for all primary γ rays from this state is determined to be $I_\gamma = 0.23^{+0.08}_{-0.07}\%$. Together with the βp intensity of $I_{p1} = 11.1(12)\%$ and the experimentally determined proton-decay partial width of $\Gamma_p = 2.9(10)$ eV in Ref. [13], the γ-decay partial width is derived to be $\Gamma_\gamma = 6.04^{+3.00}_{-2.76}$ eV using the relation $I_p/I_\gamma = \Gamma_p/\Gamma_\gamma$.

C. Shell-model calculation

The spin-parity of the $E_x = 5945.9(40)$ keV state was reported to be 0^+ by Parpottas *et al.* [17], which was concluded from the comparison of experimental cross sections with Hauser-Feshbach calculations. But it was under debate as only one 0^+ state was expected in this resonant energy region based on the mirror nuclei analysis and shell-model calculations [19–21]. In Ref. [21], Chipps suggested that a 0^+ assignment for both states is possible if one is due to cross-shell excitations. Therefore, the present work performed shell-model calculations in both the *sd* region and cross-shell excitations to investigate the spin-parity assignment of the $E_x = 5945.9(40)$ keV state.

The USD family including USD [39,40], USDA, and USDB [41] are successful Hamiltonians in the *sd* region, but they are developed for the structure of neutron-rich nuclei. If proton-rich nuclei are considered, such as ^{26}Si and ^{25}Al, the weakly bound effect of the proton $1s_{1/2}$ orbit should be included [42]. USD*, USDA*, and USDB* Hamiltonians that incorporate such an effect reasonably reproduce the mirror-energy differences in the *sd* region [42]. Recent observations on the β decay of ^{22}Si and ^{27}S show that the weakly bound effect is important to explain the decay properties and the levels of corresponding daughter nuclei [27,30]. In our calculation, all three Hamiltonians in the *sd* region, USD*, USDA*, and USDB*, give similar results for the structure of ^{26}Si, which also reproduces the experimental energy and the spin-parity of the presently considered states [14]: 5676.2(3) keV (1_1^+), 5890.1(3) keV (0_4^+), and 5929.4(8) keV (3_3^+). However, other than the 0_4^+ state, all three Hamiltonians predict that the 0_5^+ state locates at $E_x > 7.9$ MeV. Further shell-model calculations, in which the *p* to *sd* and *sd* to *pf* cross-shell excitations through the *psd* Hamiltonian YSOX [43] and the *sdpf* Hamiltonian sdpf-m [44] are considered, are performed to attempt to explain the possibility of a low-lying 0_5^+ state. However, the results show that the cross-shell excitation could not reduce the excitation energy of the 0_5^+ state to be lower than $E_x = 7.7$ MeV. Indeed, all three Hamiltonians, USD*, USDA*, and USDB*, predict a 4^+ state around $E_x = 5.8$ MeV that is consistent with the mirror-nuclei analysis [45]. Therefore, our calculations refute the existence of another 0^+ state within the interested resonance energy region, but they favor a 4^+ assignment for the 5945.9(40) keV state.

Except for the decay properties of the $E_x = 5929.4(8)$ keV state, proton- and γ-decay partial widths of other resonant states are all calculated with the abovementioned shell model with the USD* Hamiltonian in the *sd* region. Combining the observed decay energies and the shell-model $B(E2)$ and $B(M1)$ values, the γ-decay partial widths of the 5676.2(3), 5890.1(3), and 5945.9(40) keV states are calculated to be 1.17×10^{-1}, 7.71×10^{-3}, and 2.54×10^{-2} eV, respectively. To calculate the proton-decay partial width, Eq. (1) [46] can be used:

$$\Gamma_p = C^2 S_p \Gamma_{\rm sp}, \tag{1}$$

where C^2S_p is the single-particle spectroscopic factor calculated by shell model and $\Gamma_{\rm sp}$ is the single-particle partial width. In the present work, the adopted proton-decay partial widths of 5676.2(3), 5890.1(3), and 5945.9(40) keV states are calculated to be 1.24×10^{-8}, 3.86×10^{-3}, and 7.80×10^{-3} eV, respectively.

D. Astrophysical reaction rate

The total reaction rate for ^{25}Al$(p,\gamma)^{26}$Si can be expressed as the sum of all resonant and nonresonant capture contributions. For the resonant part, the reaction rate can be calculated by the well-known narrow resonance formalism [47,48]

$$N_A\langle\sigma\nu\rangle_r = 1.5394 \times 10^{11}(\mu T_9)^{-\frac{3}{2}}(\omega\gamma)\exp\left(-\frac{11.605E_r}{T_9}\right), \tag{2}$$

where $\mu = A_T/(1 + A_T)$ is the reduced mass in atomic mass units, and $A_T = 25$ is the mass number of ^{25}Al. T_9 is the

TABLE II. Present ^{25}Al$(p,\gamma)^{26}$Si resonance parameters.

J^π	E_r (keV)[a]	$\omega\gamma$ (eV)
1^+	162.2(3)	3.09×10^{-9}
0^+	376.1(3)	2.14×10^{-4}
3^+	412.4(19)[b]	$3.45^{+1.70}_{-1.57} \times 10^{-2}$
(4^+)	431.9(40)	4.48×10^{-3}

[a]Derived from databases [14,15].
[b]Error-weighted mean value from this work and Refs. [22,23].

temperature in units of GK and E_r is the resonance energy in MeV. $\omega\gamma$ is the resonance strength in MeV, which is described as

$$\omega\gamma = \frac{2J_r+1}{(2J_p+1)(2J_T+1)}\frac{\Gamma_p\Gamma_\gamma}{\Gamma_{\rm tot}}, \tag{3}$$

where J_r is the spin of resonance, $J_p = \frac{1}{2}$ is the spin of the proton, and $J_T = \frac{5}{2}$ is the spin of the ground state of ^{25}Al. Γ_p and Γ_γ are the proton and γ-ray partial widths of the resonance, respectively, and $\Gamma_{\rm tot}$ is the total width defined as $\Gamma_{\rm tot} = \Gamma_p + \Gamma_\gamma$. The adopted values of resonance strength in this work are shown in the last column of Table II.

The resonance energy E_r plays an important role in the calculation of the resonant capture reaction rate because it is exponentially related in the narrow resonance formalism [see Eq. (2)]. For the $E_x = 5929.4(8)$ keV state, the center-of-mass proton energy is measured to be 418(8) keV in this work. Combining previous measurements in Refs. [22,23], an error-weighted mean value of 412.4(19) keV is adopted here for the resonance energy. For other states, the resonance energy can be derived by the excitation energy and the reaction Q value with the relation of $E_r = E_x - Q_{p\gamma}$. Because $Q_{p\gamma}$ can be derived precisely from the database AME2016 [15] now, the uncertainties of the resonance energy are dominated by the errors in the excitation energy E_x. Here we adopt the excitation energies from the latest database [14], which are evaluated from the previous measurements, to derive the resonance energies as shown in the second column of Table II.

The nonresonant part of the ^{25}Al$(p,\gamma)^{26}$Si reaction rate can be estimated using the expression [47–49]

$$N_A\langle\sigma v\rangle_{\rm dc} = 7.8327\times10^9\left(\frac{Z_T}{\mu T_9^2}\right)^{\frac{1}{3}} S_{\rm eff} \times \exp\left[-4.2487\left(\frac{Z_T^2\mu}{T_9}\right)^{\frac{1}{3}}\right], \tag{4}$$

where μ is the reduced mass in atomic mass units and $Z_T = 13$ is the atomic number of ^{25}Al. $S_{\rm eff}$ is the effective astrophysical S factor that can be expressed by

$$S_{\rm eff} \approx S(0)\left[1 + 0.09807\left(\frac{T_9}{Z_T^2\mu}\right)^{1/3}\right], \tag{5}$$

where $S(0)$ is the S factor at zero energy [47,48,50]. In previous works, both Iliadis *et al.* [12] and Matic *et al.* [51] calculated the S factor with the value of 27 keV-b and 28 keV-b, respectively. As the Q value adopted in Matic's calculation was much closer to the derived value of $Q_{p\gamma} = 5514.0(1)$ keV by AME2016 [15], we adopt $S(0) = 28$ keV-b in Matic's work for the calculation of the nonresonant capture reaction rate. A 30% uncertainty of the nonresonant capture reaction rate is used here to estimate the upper and lower limits following Ref. [52].

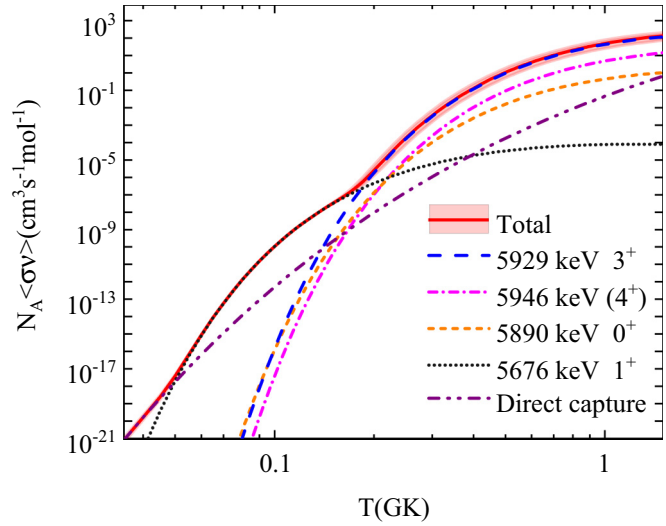

FIG. 6. Proton-capture reaction rates of ^{25}Al$(p,\gamma)^{26}$Si. The red (gray) shadow area is the upper and lower limits of the total reaction rate. Nonresonant and resonant reaction rates are presented in different colored lines.

Figure 6 presents the ^{25}Al$(p,\gamma)^{26}$Si reaction rates as a function of the stellar temperature T in units of GK. The shadow area colored in red (gray) displays the upper and lower limits of the total reaction rate. The nonresonant part makes the largest contribution to the total reaction rate when $T < 0.05$ GK. Then the $E_x = 5676.2(3)$ keV, $J^\pi = 1^+$ resonance becomes the main component of the total rate until $T \approx 0.18$ GK. In temperature range of $T > 0.18$ GK, the total reaction rate is dominated by the $E_x = 5929.4(8)$ keV, $J^\pi = 3^+$ resonance. The recently confirmed $E_x = 5890.1(3)$ keV, $J^\pi = 0^+$ resonance makes a non-negligible contribution to the total rate as temperature increases. When $T > 0.22$ GK, the $E_x = 5945.9(40)$ keV state, of which the spin-parity is assigned to be 4^+ in the discussion above, makes the secondary contribution to the total reaction rate.

Figure 7 shows the ratios of the present total reaction rate to the recommended literature values in the JINA REACLIB database [53]. The shadow parts are marked as the upper and lower limits of the total reaction rate from the present work. In high-temperature environments where the $E_x = 5929.4(8)$ keV, $J^\pi = 3^+$ resonance dominates the ^{25}Al$(p,\gamma)^{26}$Si reaction as shown in Fig. 6, the total reaction rate in this work is consistent within uncertainties with the literature values when $T > 0.20$ GK. At the temperature range of 0.05 GK $< T <$ 0.18 GK, our result is slightly larger than previous calculations because a relatively larger resonance strength of $\omega\gamma = 3.09\times10^{-9}$ eV is adopted for the $E_x = 5676.2(3)$ keV, $J^\pi = 1^+$ resonance here. At temperatures below 0.05 GK, the present work shows a consistent result

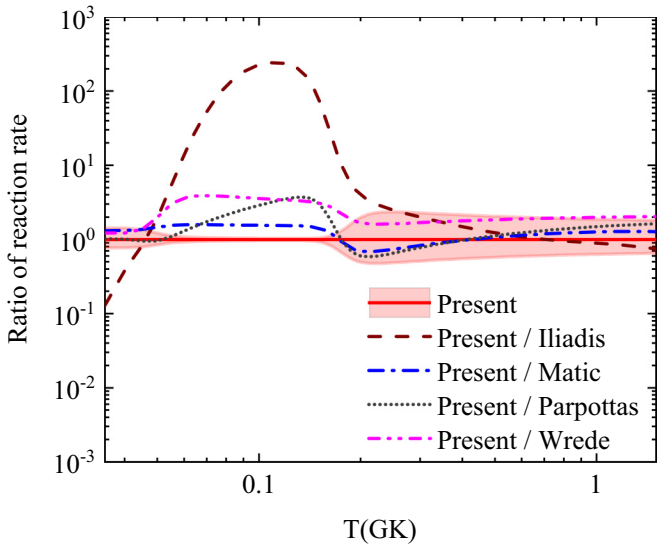

FIG. 7. Ratios of the present total ^{25}Al$(p,\gamma)^{26}$Si reaction rate to the literature values [12,16,17,51] in the JINA REACLIB database [53]. The red (gray) shadow area shows the upper and lower limits in this work.

with previous ones. It should be noticed that the present total reaction rate could not be matched to the result in Iliadis et al.'s estimation [12] at temperatures where the $E_x = 5676.2(3)$ keV, $J^\pi = 1^+$ resonance dominates the total reaction rate, because a much more accurate resonance energy of $E_r = 162.2(3)$ keV from the latest databases [14,15] is adopted here rather than the $E_r = 44(28)$ keV in the work of Iliadis *et al.* [12].

IV. CONCLUSIONS

In the present work, we performed the first simultaneous measurement of the β-delayed protons at 418(8) keV and γ rays at 1742(2) keV emitted from the astrophysically important $E_x = 5929.4(8)$ keV, $J^\pi = 3^+$ state of ^{26}Si which dominates the proton-capture reaction rate of ^{25}Al$(p,\gamma)^{26}$Si and further influences the nucleosynthesis of galactic ^{26}Al. The corresponding βp and $\beta\gamma$ intensities are measured to be $I_{p1} = 11.1(12)\%$ and $I_{\gamma 1} = 0.59(44)\%$, respectively, with a detector system consisting of a silicon array and five clover-type HPGe detectors. This simultaneous measurement could reduce the uncertainties caused by the differences in experimental setups, thus providing more reliable decay information of the $E_x = 5929.4(8)$ keV state. Moreover, shell models with weakly bound effects in the *sd* shell region were used to investigate the resonances of ^{26}Si and successfully reproduced the energy level and the spin-parity of experimental determined states at 5676.2(3) keV, $J^\pi = 1^+$; 5890.1(3) keV, $J^\pi = 0^+$; and 5929.4(8) keV, $J^\pi = 3^+$. On the other hand, shell-model calculations with three Hamiltonians, USD*, USDA*, and USDB*, in both the *sd* shell region and cross-shell excitations could not reproduce a 0_5^+ state with the excitation energy lower than $E_x = 7.7$ MeV. Indeed a 4^+ state at around $E_x = 5.8$ MeV was predicted, suggesting a 4^+ spin-parity assignment for the $E_x = 5945.9(40)$ keV state. By combining experimental results and shell-model calculations with USD* Hamiltonians in the *sd* region, we calculate the total reaction rate of ^{25}Al$(p,\gamma)^{26}$Si in explosive hydrogen burning environments. Compared with literature values in the JINA REACLIB database, our result is consistent with previous studies at $T > 0.2$ GK.

ACKNOWLEDGMENTS

We wish to acknowledge the support of the HIRFL operations staff for providing high-quality beams and the effort of the RIBLL1 collaborators in performing the experiment. This work is supported by the Ministry of Science and Technology of China under the National Key R&D Programs No. 2016YFA0400503 and No. 2018YFA0404404; the National Natural Science Foundation of China under Grants No. U1932206, No. U1632136, No. 11635015, No. 11805120, No. 11705244, No. U1432246, No. 11775316, No. U1732145, No. 11705285, No. U1867212, No. 11805280, No. 11825504, No. 11675229, and No. 11490562; the Youth Innovation Promotion Association of Chinese Academy of Sciences under Grant No. 2019406; the Continuous Basic Scientific Research Project No. WDJC-2019-13; the China Postdoctoral Science Foundation under Grants No. 2017M621442 and No. 2017M621035, and the Office of China Postdoctoral Council under the International Postdoctoral Exchange Fellowship Program (Talent-Dispatch Program) No. 20180068.

[1] W. Wang, M. G. Lang, R. Diehl, H. Halloin, P. Jean, J. Knödlseder, K. Kretschmer, P. Martin, J. P. Roques, A. W. Strong, C. Winkler, and X. L. Zhang, Astron. Astrophys. **496**, 713 (2009).

[2] R. Diehl, H. Halloin, K. Kretschmer, G. G. Lichti, V. Schönfelder, A. W. Strong, A. von Kienlin, W. Wang, P. Jean, J. Knödlseder, J.-P. Roques, G. Weidenspointner, S. Schanne, D. H. Hartmann, C. Winkler, and C. Wunderer, Nature (London) **439**, 45 (2006).

[3] J. Knödlseder, K. Bennett, H. Bloemen, R. Diehl, W. Hermsen, U. Oberlack, J. Ryan, V. Schönfelder, and P. von Ballmoos, Astron. Astrophys. **344**, 68 (1999).

[4] S. Plüschke, R. Diehl, V. Schönfelder, H. Bloemen, W. Hermsen, K. Bennett, C. Winkler, M. McConnell, J. Ryan, U. Oberlack, and J. Knödlseder, in *Exploring the Gamma-Ray Universe*, edited by A. Gimenez, V. Reglero, and C. Winkler, ESA Special Publication, Vol. 459 (ESA, Noordwijk, The Netherlands, 2001), pp. 55–58.

[5] D. Smith, New Astron. Rev **48**, 87 (2004).

[6] M. J. Harris, J. Knödlseder, P. Jean, E. Cisana, R. Diehl, G. G. Lichti, J.-P. Roques, S. Schanne, and G. Weidenspointner, Astron. Astrophys. **433**, L49 (2005).

[7] T. Rauscher, A. Heger, R. D. Hoffman, and S. E. Woosley, Astrophys. J. **576**, 323 (2002).

[8] S. Woosley and A. Heger, Phys. Rep. **442**, 269 (2007).
[9] A. Parikh, J. José, and G. Sala, AIP Adv. **4**, 041002 (2014).
[10] J. José, M. Hernanz, and A. Coc, Astrophys. J. **479**, L55 (1997).
[11] M. B. Bennett *et al.*, Phys. Rev. Lett. **111**, 232503 (2013).
[12] C. Iliadis, L. Buchmann, P. M. Endt, H. Herndl, and M. Wiescher, Phys. Rev. C **53**, 475 (1996).
[13] P. N. Peplowski, L. T. Baby, I. Wiedenhöver, S. E. Dekat, E. Diffenderfer, D. L. Gay, O. Grubor-Urosevic, P. Höflich, R. A. Kaye, N. Keeley, A. Rojas, and A. Volya, Phys. Rev. C **79**, 032801(R) (2009).
[14] M. Basunia and A. Hurst, Nucl. Data Sheets **134**, 1 (2016).
[15] M. Wang, G. Audi, F. Kondev, W. Huang, S. Naimi, and X. Xu, Chin. Phys. C **41**, 030003 (2017).
[16] C. Wrede, Phys. Rev. C **79**, 035803 (2009).
[17] Y. Parpottas, S. M. Grimes, S. Al-Quraishi, C. R. Brune, T. N. Massey, J. E. Oldendick, A. Salas, and R. T. Wheeler, Phys. Rev. C **70**, 065805 (2004).
[18] D. W. Bardayan, J. A. Howard, J. C. Blackmon, C. R. Brune, K. Y. Chae, W. R. Hix, M. S. Johnson, K. L. Jones, R. L. Kozub, J. F. Liang, E. J. Lingerfelt, R. J. Livesay, S. D. Pain, J. P. Scott, M. S. Smith, J. S. Thomas, and D. W. Visser, Phys. Rev. C **74**, 045804 (2006).
[19] D. T. Doherty, P. J. Woods, D. Seweryniak, M. Albers, A. D. Ayangeakaa, M. P. Carpenter, C. J. Chiara, H. M. David, J. L. Harker, R. V. F. Janssens, A. Kankainen, C. Lederer, and S. Zhu, Phys. Rev. C **92**, 035808 (2015).
[20] T. Komatsubara, S. Kubono, T. Hayakawa, T. Shizuma, A. Ozawa, Y. Ito, Y. Ishibashi, T. Moriguchi, H. Yamaguchi, D. Kahl, S. Hayakawa, D. Nguyen Binh, A. A. Chen, J. Chen, K. Setoodehnia, and T. Kajino, Eur. Phys. J. A **50**, 136 (2014).
[21] K. A. Chipps, Phys. Rev. C **93**, 035801 (2016).
[22] Ł. Janiak *et al.*, Phys. Rev. C **95**, 034315 (2017).
[23] J.-C. Thomas, L. Achouri, J. Äystö, R. Béraud, B. Blank, G. Canchel, S. Czajkowski, P. Dendooven, A. Ensallem, J. Giovinazzo, N. Guillet, J. Honkanen, A. Jokinen, A. Laird, M. Lewitowicz, C. Longour, F. de Oliveira Santos, K. Peräjärvi, and M. Stanoiu, Eur. Phys. J. A **21**, 419 (2004).
[24] W. Zhan, J. Xia, H. Zhao, G. Xiao, Y. Yuan, H. Xu, K. Man, P. Yuan, D. Gao, X. Yang, M. Song, X. Cai, X. Yang, Z. Sun, W. Huang, Z. Gan, and B. Wei, Nucl. Phys. A **805**, 533c (2008).
[25] Z. Sun, W.-L. Zhan, Z.-Y. Guo, G. Xiao, and J.-X. Li, Nucl. Instrum. Methods Phys. Res., Sect. A **503**, 496 (2003).
[26] L. Sun *et al.*, Nucl. Instrum. Methods Phys. Res., Sect. A **804**, 1 (2015).
[27] L. J. Sun *et al.* (RIBLL Collaboration), Phys. Rev. C **99**, 064312 (2019).
[28] L. J. Sun, X. X. Xu, S. Q. Hou, C. J. Lin, J. José, J. Lee, J. J. He, Z. H. Li, J. S. Wang, C. X. Yuan *et al.*, Phys. Lett. B **802**, 135213 (2020).
[29] S. Li-Jie, L. Cheng-Jian, X. Xin-Xing, W. Jian-Song, J. Hui-Ming, Y. Feng, Y. Yan-Yun, Y. Lei, B. Peng-Fei, Z. Huan-Qiao, J. Shi-Lun, W. Zhen-Dong, Z. Ning-Tao, C. Si-Ze, M. Jun-Bing, M. Peng, M. Nan-Ru, and L. Zu-Hua, Chin. Phys. Lett. **32**, 012301 (2015).
[30] X. Xu *et al.*, Phys. Lett. B **766**, 312 (2017).
[31] L. J. Sun *et al.*, Phys. Rev. C **95**, 014314 (2017).
[32] K. Wang *et al.*, Int. J. Mod. Phys. E **27**, 1850014 (2018).
[33] Y.-T. Wang *et al.*, Eur. Phys. J. A **54**, 107 (2018).
[34] X.-X. Xu, F. C. E. Teh, C.-J. Lin, J. Lee, F. Yang, Z.-Q. Guo, T.-S. Guo, L.-J. Sun, X.-Z. Teng, J.-J. Liu, P.-J. Li, P.-F. Liang, L. Yang, N.-R. Ma, H.-M. Jia, D.-X. Wang, S. Leblond, T. Lokotko, Q.-Q. Zhao, and H.-Q. Zhang, Nucl. Sci. Technol. **29**, 73 (2018).
[35] J. Görres, M. Wiescher, K. Scheller, D. J. Morrissey, B. M. Sherrill, D. Bazin, and J. A. Winger, Phys. Rev. C **46**, R833(R) (1992).
[36] W. Trinder, E. Adelberger, B. Brown, Z. Janas, H. Keller, K. Krumbholz, V. Kunze, P. Magnus, F. Meissner, A. Piechaczek, M. Pfützner, E. Roeckl, K. Rykaczewski, W.-D. Schmidt-Ott, and M. Weber, Nucl. Phys. A **620**, 191 (1997).
[37] D. Pérez-Loureiro *et al.*, Phys. Rev. C **93**, 064320 (2016).
[38] N. L. Achouri, F. de Oliveira Santos, M. Lewitowicz, B. Blank, J. Äystö, G. Canchel, S. Czajkowski, P. Dendooven, A. Emsallem, J. Giovinazzo, N. Guillet, A. Jokinen, A. M. Laird, C. Longour, K. Peräjärvi, N. Smirnova, M. Stanoiu, and J. C. Thomas, Eur. Phys. J. A **27**, 287 (2006).
[39] B. Wildenthal, Prog. Part. Nucl. Phys. **11**, 5 (1984).
[40] B. A. Brown and B. H. Wildenthal, Annu. Rev. Nucl. Part. Sci. **38**, 29 (1988).
[41] B. A. Brown and W. A. Richter, Phys. Rev. C **74**, 034315 (2006).
[42] C. Yuan, C. Qi, F. Xu, T. Suzuki, and T. Otsuka, Phys. Rev. C **89**, 044327 (2014).
[43] C. Yuan, T. Suzuki, T. Otsuka, F. Xu, and N. Tsunoda, Phys. Rev. C **85**, 064324 (2012).
[44] Y. Utsuno, T. Otsuka, T. Mizusaki, and M. Honma, Phys. Rev. C **60**, 054315 (1999).
[45] W. A. Richter, B. A. Brown, A. Signoracci, and M. Wiescher, Phys. Rev. C **83**, 065803 (2011).
[46] C. Iliadis, *Nuclear Physics of Stars* (Wiley, New York, 2008).
[47] C. E. Rolfs and W. S. Rodney, *Cauldrons in the Cosmos* (University of Chicago, Chicago, 1988).
[48] J. J. He, A. Parikh, Y. Xu, Y. H. Zhang, X. H. Zhou, and H. S. Xu, Phys. Rev. C **96**, 045801 (2017).
[49] H. Herndl, J. Görres, M. Wiescher, B. A. Brown, and L. Van Wormer, Phys. Rev. C **52**, 1078 (1995).
[50] W. A. Fowler, G. R. Caughlan, and B. A. Zimmerman, Annu. Rev. Astron. Astrophys. **5**, 525 (1967).
[51] A. Matic *et al.*, Phys. Rev. C **82**, 025807 (2010).
[52] C. Iliadis, J. M. D'Auria, S. Starrfield, W. J. Thompson, and M. Wiescher, Astrophys. J., Suppl. Ser. **134**, 151 (2001).
[53] R. H. Cyburt, A. M. Amthor, R. Ferguson, Z. Meisel, K. Smith, S. Warren, A. Heger, R. D. Hoffman, T. Rauscher, A. Sakharuk, H. Schatz, F. K. Thielemann, and M. Wiescher, Astrophys. J., Suppl. Ser. **189**, 240 (2010).